Retinylidene Ligand Structure in Bovine Rhodopsin, Metarhodopsin-I, and 10-Methylrhodopsin from Internuclear Distance Measurements Using ^{13}C-Labeling and 1-D Rotational Resonance MAS NMR†

P. J. E. Verdegem,‡,§ P. H. M. Bovee-Geurts,|| W. J. de Grip,|| J. Lugtenburg,‡ and H. J. M. de Groot*,‡

Leiden Institute of Chemistry, Gorlaeus Laboratories, P.O. Box 9502, 2300 RA Leiden, The Netherlands, and Department of Biochemistry & Institute of Cellular Signaling, University of Nijmegen, P.O. Box 9101, 6500 HB Nijmegen, The Netherlands

Received December 22, 1998; Revised Manuscript Received March 30, 1999

ABSTRACT: Rhodopsin is the G-protein coupled photoreceptor that initiates the rod phototransduction cascade in the vertebrate retina. Using specific isotope enrichment and magic angle spinning (MAS) NMR, we examine the spatial structure of the C10−C11═C12−C13−C20 motif in the native retinylidene chromophore, its 10-methyl analogue, and the predischarge photoproduct metarhodopsin-I. For the rhodopsin study 11-*Z*-[10,20-$^{13}C_2$]- and 11-*Z*-[11,20-$^{13}C_2$]-retinal were synthesized and incorporated into bovine opsin while maintaining a natural lipid environment. The ligand is covalently bound to Lys_{296} in the photoreceptor. The C10−C20 and C11−C20 distances were measured using a novel 1-D CP/MAS NMR rotational resonance experimental procedure that was specifically developed for the purpose of these measurements [Verdegem, P. J. E., Helmle, M., Lugtenburg, J., and de Groot, H. J. M. (1997) *J. Am. Chem. Soc. 119*, 169]. We obtain $r_{10,20} = 0.304 \pm 0.015$ nm and $r_{11,20} = 0.293 \pm 0.015$ nm, which confirms that the retinylidene is 11-*Z* and shows that the C10−C13 unit is conformationally twisted. The corresponding torsional angle is about 44° as indicated by Car−Parrinello modeling studies. To increase the nonplanarity in the chromophore, 11-*Z*-[10,20-$^{13}C_2$]-10-methylretinal and 11-*Z*-[(10-CH_3),13-$^{13}C_2$]-10-methylretinal were prepared and incorporated in opsin. For the resulting analogue pigment $r_{10,20} = 0.347 \pm 0.015$ nm and $r_{(10-CH_3),13} = 0.314 \pm 0.015$ nm were obtained, consistent with a more distorted chromophore. The analogue data are in agreement with the induced fit principle for the interaction of opsin with modified retinal chromophores. Finally, we determined the intraligand distances $r_{10,20}$ and $r_{11,20}$ also for the photoproduct metarhodopsin-I, which has a relaxed all-*E* structure. The results ($r_{10,20} \geq 0.435$ nm and $r_{11,20} = 0.283 \pm 0.015$ nm) fully agree with such a relaxed all-*E* structure, which further validates the 1-D rotational resonance technique for measuring intraligand distances and probing ligand structure. As far as we are aware, these results represent the first highly precise distance determinations in a ligand at the active site of a membrane protein. Overall, the MAS NMR data indicate a tight binding pocket, well defined to bind specifically only one enantiomer out of four possibilities and providing a steric complement to the chromophore in an ultrafast (∼200 fs) isomerization process.

Rhodopsin is the 40 kDa G-protein coupled photoreceptor that initiates the visual signal transduction cascade upon excitation with light. It is an integral membrane protein of 348 amino acids that is folded into seven transmembrane helical segments connected by extramembraneous hydrophilic loops (*1*−*7*). The photoactive site contains an 11-*Z* retinylidene chromophore covalently bound via a protonated Schiff base to lysine-296. Capture of a photon by rhodopsin initiates a photochemical reaction, in which the 11-*Z* chromophore isomerizes to a distorted all-*E* configuration (*8*). This primary step in the visual process is completed within ∼200 fs (*9*).

A central issue in the studies of the primary step in visual signal transduction is to resolve the basic molecular mechanisms that facilitate the ultrafast and efficient photochemical isomerization of the C10−C11═C12−C13−C20 moiety. In the ground state of the chromophore, the positive charge of the protonated Schiff base is partly delocalized into the polyene chain and distributed over odd-numbered carbons at the Schiff base end (*10*). Due to nonbonded interactions between 13-CH_3 and 10-H the chromophore of rhodopsins is twisted in the C10−C11═C12−C13−C20 moiety. Systems in which the torsion in this part of the molecule has been changed by differences in methyl substitution have been prepared and studied. The degree of twist in this part of the chromophore contributes to the rate and efficiency of the primary photochemical step, e.g. 13-demethylrhodopsin that has a more planar chromophore has a lower quantum yield ($\Phi = 0.47$ vs 0.67 for rhodopsin) and a formation time for

† This research was financed in part by Biotechnology Grant Bio2 CT-930467 of the European Union and by The Netherlands Organization for Scientific Research, through The Netherlands Foundation for Chemical Research (NWO-SON). H.J.M.d.G. is a recipient of a NWO PIONIER fellowship.

* Corresponding author.
‡ Leiden Institute of Chemistry.
§ Present address: Department of Radiology, University Hospital Nijmegen, P.O. Box 9101, 6500 HB Nijmegen, The Netherlands.
|| University of Nijmegen.

10.1021/bi983014e CCC: $18.00
Published on Web 08/10/1999

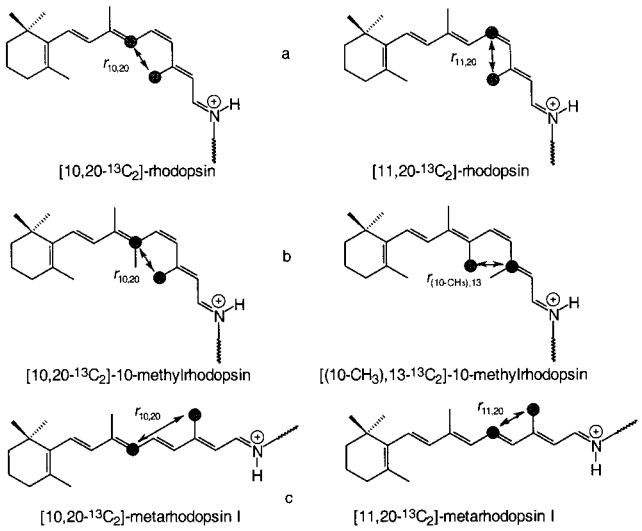

FIGURE 1: Chromophore structures and labeling patterns in (a) rhodopsin, (b) 10-methylrhodopsin, and (c) metarhodopsin-I. The filled circles indicate the position of the ^{13}C labels. The arrows represent the intraligand distances.

its batho form of 400 fs, twice that of rhodopsin (*11*). Comparison of 10-methylrhodopsin and 10-methyl-13-demethylrhodopsin also suggests a relation between torsion and quantum yield ($\Phi = 0.55$ and 0.33, respectively.) (*11*,*12*).

To provide a sound basis for such model studies and calculations, exact structural information is essential. To date such detailed information is completely lacking for eukaryotic membrane receptors, including the G-protein coupled receptor family to which rhodopsin belongs. In the present work we aim at forging a pathway to such a solid structural basis. The spatial and electronic structure of the out-of-plane distortion and the effect of the protein environment will be examined for rhodopsin and for the 10-methylrhodopsin analogue that was designed to increase the nonplanarity of the chromophore. The ligand structure and its chemical environment are characterized by measuring chemical shifts, line widths and critical intramolecular distances with CP/MAS NMR[1] using $^{13}C_2$-labeled 11-*Z*-retinals as rhodopsin chromophore.

At present there is no high-resolution structure available for rhodopsin or the retinylidene ligand bound to the receptor. Solid-state NMR in conjunction with selective isotope enrichment can already provide genuine structure information at atomic resolution for intrinsic membrane proteins that are not yet accessible to X-ray or other diffraction techniques (*13*−*15*). We will demonstrate that a recently introduced 1-D rotational resonance approach between an sp^3 and an sp^2 carbon atom (*16*) can be used to measure interatomic distances between isotope labels with good accuracy, for the retinylidene ligand in rhodopsin, for its predischarge meta-I photointermediate, and for the C10-methyl rhodopsin analogue.

For rhodopsin the focus is on the C10−C20 and C11−C20 distances in the chromophore, $r_{10,20}$ and $r_{11,20}$, respectively. Figure 1a depicts the retinylidene chromophore of [10,20-$^{13}C_2$]-rhodopsin and [11,20-$^{13}C_2$]-rhodopsin. The filled circles represent the positions of the ^{13}C labels. The structure of the chromophore of 10-methylrhodopsin is presented in Figure 1b. To study the out-of-plane distortion for the C10 methyl analogue and to establish the structural difference with the native rhodopsin, the C10−C20 and the (10-CH_3)−C13 internuclear distances, $r_{10,20}$ and $r_{(10-CH_3),13}$, were measured.

Since the ^{13}C-labeled samples are biologically fully functional, the photocascade will be triggered by illumination and the predischarge photoproduct metarhodopsin-I can be accumulated. Figure 1c represents the structures of the [10,20-$^{13}C_2$] and the [11,20-$^{13}C_2$] chromophore in metarhodopsin-I. The distance measurements in the chromophore of this intermediate confirm the structural relaxation of the chromophore after decay of the batho photoproduct and confirm the validity of the novel 1-D rotational resonance approach. This technique can be equally well extended to probe ligand structure in other G-protein coupled receptors and basically in any other membrane protein.

MATERIALS AND METHODS

The synthesis of all-*E*-[10,20-$^{13}C_2$]-retinal and all-*E*-[11,20-$^{13}C_2$]-retinal was performed using procedures originally developed by Groesbeek et al. (*17*), starting from commercially available [1-^{13}C]-acetonitrile, [2-^{13}C]-acetonitrile and [^{13}C]-methyl iodide (Cambridge Isotope Laboratories, Cambridge, MA). For the synthesis of [10,20-$^{13}C_2$]-10-methylretinal and [(10-CH_3),13-$^{13}C_2$]-10-methylretinal we developed an α-functionalization reaction for 3-methylbutenenitriles, which are published in detail elsewhere (*18*). The all-*E*-retinals were isolated by silica gel column chromatography and subsequently irradiated in dry acetonitrile and in a dry nitrogen atmosphere for 16 h using a 100 W tungsten incandescent lamp. From the resulting photostationary mixture the 11-*Z* isomers were purified with preparative HPLC, using a Zorbax silica gel column (21.2 mm × 25 cm; Du Pont, Experimental DE). The purity of the labeled retinals was confirmed with 300 MHz ^1H NMR ($CDCl_3$), 75.4 MHz ^1H-noise-decoupled ^{13}C NMR ($CDCl_3$) and mass spectrometry. The incorporation is better than 99% for every individual label. All manipulations with isomerically pure retinals and rhodopsins were performed in dim red light ($\lambda > 620$ nm) or in the dark.

For each NMR sample approximately 50 bovine retinas were dissected from fresh cow eyes, within 4 h after death. Membrane fragments containing opsin, the apoprotein of rhodopsin, were purified and regenerated with 11-*Z*-retinal or 11-*Z*-10-methylretinal following published procedures (*19*). A 2-fold excess of the doubly labeled retinal was used to obtain optimal regeneration during 1 h of incubation. The excess retinal was converted to the retinal oxime by treatment with hydroxylamine and removed by washing the rhodopsin suspension twice with a 50 mM β-cyclodextrin solution (*12*). The percentage of regeneration was deduced from the A_{280}/A_{500} ratio measured with optical spectroscopy. It was the same for parallel regenerations with labeled and unlabeled 11-*Z*-retinal and varied between 90 and 95%. NMR samples containing ~20 mg of labeled rhodopsin were concentrated to ~1 mM by centrifugation and loaded into 4 mm zirconium oxide rotors that were sealed with a boronitride cap. For the regeneration of opsin with the 11-*Z*-[10,20-$^{13}C_2$]-10-methyl-

[1] Abbreviations: CP, cross-polarization; CW, continuous wave; FID, free induction decay; MAS, magic angle spinning; NMR, nuclear magnetic resonance; TMS, tetramethylsilane; MD, molecular dynamics.

retinal or 11-*Z*-[(10-CH_3),13-$^{13}C_2$]-retinal a 3-fold excess of pure 11-*Z*-10-methylretinal was added to a suspension containing opsin. Complete regeneration takes considerably longer than for retinal and was performed overnight (*12*).

CP/MAS NMR experiments were performed overnight with a Bruker MSL 400 spectrometer operating with a ^{13}C frequency of 100.6 MHz, using a 4 mm MAS probe with infrared spinning speed detection. Ramped cross polarization and CW decoupling with a nutation frequency of ~80 kHz in the proton channel were used (*20*). The protein spectra were collected from frozen samples at a temperature of ~210 K. To allow for stable high-speed spinning, the cooling was performed by leading the bearing nitrogen gas through a pressurized liquid nitrogen bath. For the rotational resonance distance measurements, the spinning speed was maintained within ~3 Hz of the rotational resonance condition. Approximately 25 000 transients were accumulated with a recycle delay of 1.75 s. The data were collected in 4K points with a digital resolution of 12 Hz. Prior to Fourier transformation, the FID's were zero-filled to 8K points. All NMR data are externally referenced to the 1-^{13}C of singly labeled glycine, which resonates at 176.04 ppm downfield from TMS.

For the accumulation of the metarhodopsin-I intermediate, the NMR rotors were immersed in liquid nitrogen and illuminated with a 500 W xenon lamp. After ~10 h of illumination, the sample was transferred to the cold NMR probe (−20 °C). During illumination rhodopsin is partially converted to bathorhodopsin (*21*). The bathorhodopsin is metastable below −143 °C and can be trapped at liquid nitrogen temperatures (*22*, *23*). Subsequent heating to −20 °C yields a mixture of rhodopsin and metarhodopsin-I. The reduced lipid content of the sample due to the cyclodextrin extraction was an additional precaution that the photosequence of these samples does not proceed beyond the metarhodopsin at the metarhodopsin-I stage (*12*, *20*, *24*, *25*). In this way typically 70% conversion to metarhodopsin-I can be obtained. After the NMR experiments were finished, the metarhodopsin-I sample was investigated with UV−VIS spectroscopy. The spectrum presented a main absorbance band with $\lambda_{max} = 478$ nm, typical for metarhodopsin-I, with a small shoulder at $\lambda = 500$ nm originating from the remaining rhodopsin in the sample (spectra not shown). This confirms that the analyzed photoproduct represents metarhodopsin-I.

RESULTS

In a rotational resonance experiment the interference of the MAS with the homonuclear dipole interactions within a pair of nuclear magnetic moments is utilized for the determination of internuclear distances through-space (*26*, *27*). At the $n = 1$ rotational resonance condition, when ω_r matches the difference in resonance frequency $\Delta\omega_{IS}$ of the two ^{13}C nuclei, the line shapes change and additional fine structure or broadening can be observed for internuclear distances up to ~0.4 nm (*16*). When the transverse relaxation properties and inhomogeneous line widths are favorable, the fine structure due to the rotational resonance effect can be resolved and a "splitting" of the resonance $\Delta\omega_1$ is detected. $\Delta\omega_1$ can be extracted, for instance, by taking the second derivative of the data with respect to the frequency. It has been verified that the following linear relation exists between the dipolar coupling constant b_{IS} and $\Delta\omega_1$

$$\frac{b_{IS}}{2\pi\sqrt{8}} = a_1 \frac{\Delta\omega_1}{2\pi} + a_0 \qquad (1)$$

to a good approximation, with $a_1 = 1.15$ and a_0 a small offset, depending on the experimental line width (*16*).

From the dipolar coupling constant the internuclear distance r_{IS} can be calculated:

$$b_{IS} = \left|-\left(\frac{\mu_0}{4\pi}\right)\frac{\gamma^2\eta}{r_{IS}^{\ 3}}\right| \qquad (2)$$

Equation 1 summarizes the variation of $\Delta\omega_1$ with b_{IS} in a series of numerical simulations for a homonuclear two spin system at the $n = 1$ rotational resonance condition, taking into account the dipolar interaction, shift anisotropy, and a pseudo transverse relaxation parameter (*16*). In eq 2 μ_0 is the magnetic permeability in a vacuum, γ is the gyromagnetic ratio of the ^{13}C nuclei, and r_{IS} represents the internuclear distance. It has been demonstrated for [10,20-$^{13}C_2$]-, [11,20-$^{13}C_2$]- and [12,20-$^{13}C_2$]-retinal polycrystalline powders that C10−C20, C11−C20, and C12−C20 internuclear distances can be extracted with good accuracy from a straightforward measurement of the $\Delta\omega_1$ in the vinylic response (*16*).

The specific aim of this investigation is to determine the structure of the C10−C11═C12−C13−C20 moiety of the chromophores in rhodopsin, 10-methylrhodopsin, and metarhodopsin-I, using the same 1-D rotational resonance strategy as used previously for the retinal models to measure internuclear distances. 11-*Z* retinal specifically enriched in pairs of ^{13}C nuclei was incorporated into rhodopsin. Except for the metarhodopsin data presented in Figure 5, we have applied exponential apodizations of 40 Hz prior to Fourier transformation. Since the a_0 in eq 1 depends on the experimental line width after Fourier transformation, the effect of the apodization was analyzed with computer simulations of the homonuclear spin pair response for a range of dipolar couplings. It appears that for the rhodopsin rotational resonance spectra the total line width including apodization is 110 Hz. Using the simulation procedures that were established earlier for the calibration of the retinal data (*16*), an offset $a_0 = 12$ Hz was determined, independent of $b_{IS}/(2\pi\sqrt{8})$.

The distance information obtained from the 1-D rotational resonance MAS NMR is considerably more accurate than the structural information available thus far from electron diffraction studies (*4*, *5*), NMR shift constraints (*28*), and the interpretation of resonance Raman and FTIR data (*29*). Since $r_{IS} \propto \Delta\omega_1^{-3}$, the typical experimental error of ~7 Hz associated with $\Delta\omega_1$ allows the measurement of distances with a good error margin of ±0.015 nm, which represents the statistical error of the measurement (*16*).

Rhodopsin. Figure 2a represents the natural abundance ^{13}C CP/MAS NMR spectrum for rhodopsin. The data were collected with $\omega_r/2\pi = 7000$ Hz and are characteristic for an intrinsic membrane protein. Between 0 and 70 ppm, the saturated carbon signals for the protein residues and the lipids are observed. A broad spectral feature around 125 ppm is from resonances associated with the unsaturated carbons of phospholipids in the natural bilayer membrane and the

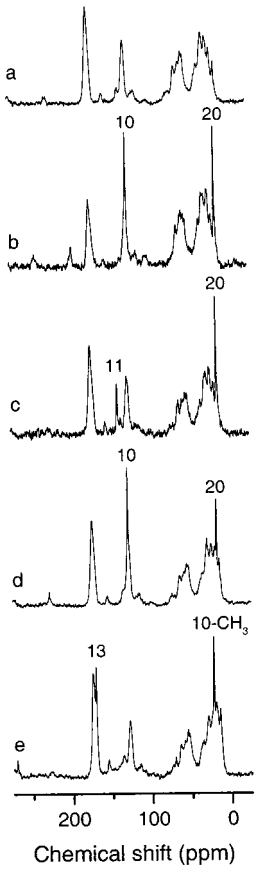

FIGURE 2: 100.6 MHz CP/MAS NMR spectra of (a) natural abundance rhodopsin with $\omega_r/2\pi = 7000$ Hz, (b) [10,20-$^{13}C_2$]-rhodopsin with $\omega_r/2\pi = 7000$ Hz, and (c) [11,20-$^{13}C_2$]-rhodopsin, collected with $\omega_r/2\pi = 10\,000$ Hz, (d) [10,20-$^{13}C_2$]-10-methylrhodopsin and (e) [(10-CH_3),13-$^{13}C_2$]-10-methylrhodopsin. The analogue data were collected off rotational resonance with $\omega_r/2\pi = 10\,000$ Hz. The tags indicate the various label resonances.

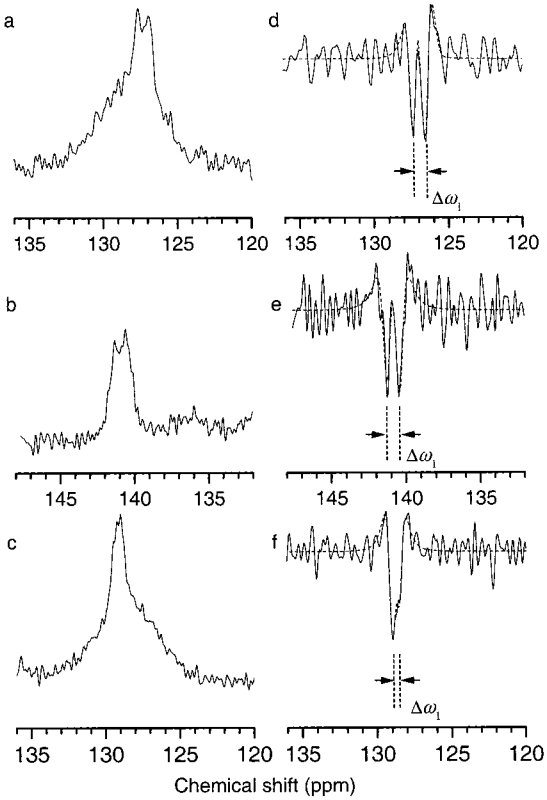

FIGURE 3: Left: (a) Vinylic region of the 100.6 MHz CP/MAS NMR spectrum of [10,20-$^{13}C_2$]-rhodopsin, collected at the $n = 1$ rotational resonance condition of $\omega_r/2\pi = 11\,794 \pm 3$ Hz; (b) vinylic data for [11,20-$^{13}C_2$]-rhodopsin, at the $n = 1$ rotational resonance condition, with $\omega_r/2\pi = 12592 \pm 3$ kHz; (c) vinylic data for [10,20-$^{13}C_2$]-10-methylrhodopsin, also at $n = 1$ rotational resonance, with $\omega_r/2\pi = 10230 \pm 3$ Hz. Right**:** Vinylic regions of the second derivative signals of (d) [10,20-$^{13}C_2$]-rhodopsin, (e) [11,20-$^{13}C_2$]-rhodopsin, and (f) [10,20-$^{13}C_2$]10-methylrhodopsin. The smooth dashed curves represent the deconvolution with pairs of second derivatives of Lorentzian lines. The vertical dashed lines indicate the measured apparent splitting $\Delta\omega_1$.

aromatic side chains of the protein. The response around 175 ppm, with weak MAS sidebands at 105 and 245 ppm, represents the signals from peptide carbonyl and lipid ester ^{13}C nuclei.

For each doubly ^{13}C-labeled rhodopsin sample a data set well off rotational resonance was collected ([10,20-$^{13}C_2$]-rhodopsin at $\omega_r/2\pi = 7000$ Hz, Figure 2b; [11,20-$^{13}C_2$]-rhodopsin at $\omega_r/2\pi = 10\,000$ Hz, Figure 2c). In Figure 2b the resonances from the label pair are clearly visible with $\sigma = 127.3$ ppm for the vinylic C10 position and $\sigma = 15.8$ ppm for the methyl C20 resonance, in close agreement with the values of 127.8 and 16.8 ppm reported by Smith et al. for rhodopsin in detergent micelles (*29*). The C10 response gives rise to weak sidebands at 57.3 and 197.3 ppm. The centerband resonances were analyzed using Lorentzians to determine $\Delta\omega_{IS}$ and the experimental line width. For the [10,20-$^{13}C_2$]-rhodopsin the $n = 1$ rotational resonance condition is $\omega_r/2\pi = 11\,794 \pm 3$ Hz. Figure 2c shows the C11 response at $\sigma = 140.9$ ppm, close to the $\sigma = 141.6$ ppm for the detergent-solubilized rhodopsin (*29*), and the C20 resonance again at $\sigma = 15.8$ ppm. This gives $\omega_r/2\pi = 12\,592 \pm 3$ Hz for the $n = 1$ rotational resonance condition. Due to zero-filling and the interpolation by the Lorentzian fitting procedure, the estimated accuracy is ~3 Hz.

Figure 3 shows the vinylic regions of the CP/MAS NMR spectra of [10,20-$^{13}C_2$]-rhodopsin (a) and [11,20-$^{13}C_2$]-rhodopsin (b) at their respective $n = 1$ rotational resonance conditions. In both spectra the signals from the vinylic labels are split due to the rotational resonance dipolar recoupling effect (*30*). Using the second derivative procedure that was established for the retinal model compounds, the $\Delta\omega_1$ can be determined (Figure 3) (*16*). This yields $\Delta\omega_1/2\pi = 73 \pm 7$ Hz for [10,20-$^{13}C_2$]-rhodopsin and $\Delta\omega_1/2\pi = 82 \pm 7$ Hz for [11,20-$^{13}C_2$]-rhodopsin. To estimate the error margins of this fitting process, we employed the following procedure. After the optimal fit with two Lorentzians as shown in Figure 3, the data and fit were superimposed again but with an overestimation and underestimation of $\Delta\omega_1/2\pi$ of 1, 5, and 10 Hz, as shown in Figure 4. The differences between the "fits" and the data are indicated below the graphs, together with the standard deviation of the resulting noise. It is clear that when the deviation between the optimal fit and the position of the Lorenzians increases, the mismatch between the simulations and data becomes more prominent. We estimate that an error margin of ±7 Hz is appropriate to our fit procedure.

The $\Delta\omega_1$ can be used to calculate the C10−C20 and C11−C20 scaled dipolar coupling constants (eq 1 with $a_0 = 12$ Hz), $b_{10,20}/(2\pi\sqrt{8}) = 96 \pm 7$ Hz, and $b_{11,20}/(2\pi\sqrt{8}) = 106 \pm 7$ Hz, respectively. The internuclear distances, calculated

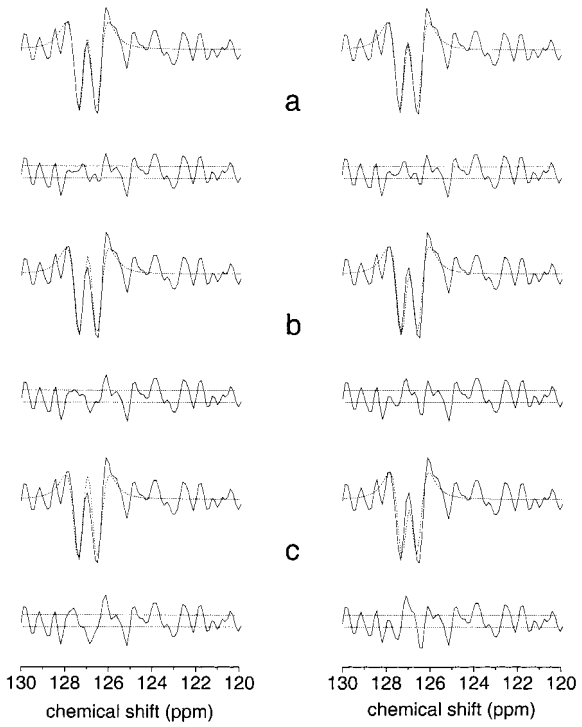

FIGURE 4: Comparisons of the second derivative data of the $n = 1$ rotational resonance spectrum of [10,20-$^{13}C_2$]-rhodopsin and the fit with the two second derivative Lorentzians but with an overestimation and underenstimation of $\Delta\omega_1/2\pi$ by 1 (a), 5 (b), and 10 Hz (c), relative to the optimum. The differences between fit and data are depicted under the graphs, together with the standard deviation of the noise.

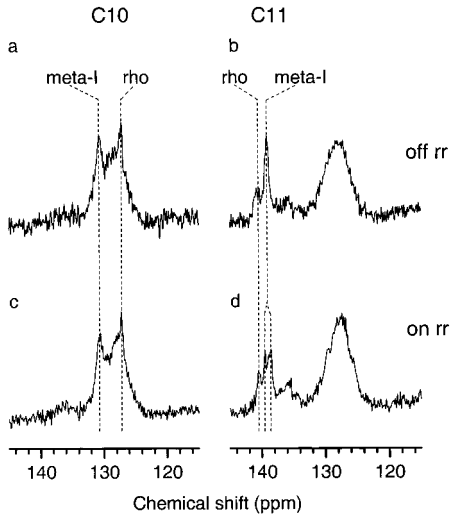

FIGURE 5: Vinylic regions of the off rotational resonance and $n = 1$ rotational resonance spectra of (a) [10,20-$^{13}C_2$]-metarhodopsin-I and (b) [11,20-$^{13}C_2$]-metarhodopsin-I. The off rotational resonance spectra were collected at $\omega_r/2\pi = 10000$ Hz. The $n = 1$ rotational resonance spectrum for [10,20-$^{13}C_2$]-metarhodopsin-I was collected at $\omega_r/2\pi = 11810 \pm 3$ Hz (c). The $n = 1$ rotational resonance spectrum for [11,20-$^{13}C_2$]-metarhodopsin-I was collected at $\omega_r/2\pi = 12689 \pm 3$ Hz (d). The vertical dashed lines show the isotropic shifts of the label resonances in rhodopsin and metarhodopsin-I (a−c) and the splitting that was observed for the $n = 1$ rotational resonance spectrum for [11,20-$^{13}C_2$]-metarhodopsin-I (d).

from eq 2, are $r_{10,20} = 0.304 \pm 0.015$ nm and $r_{11,20} = 0.293 \pm 0.015$ nm (Table 1).

10-Methylrhodopsin. The CP/MAS spectra of natural abundance 10-methylrhodopsin, [10,20-$^{13}C_2$]-10-methylrhodopsin, and [(10-CH_3),13-$^{13}C_2$]-10-methylrhodopsin, were collected with $\omega_r/2\pi = 10\,000$ Hz (spectra shown in Figure 2d,e). The C20 response in [10,20-$^{13}C_2$]-10-methylrhodopsin is at 17.4 ppm, shifted downfield by 1.6 ppm compared to the C20 signal from rhodopsin. The vinylic C10 carbon resonates with $\sigma = 129.2$ ppm, downfield shifted by 1.9 ppm relative to rhodopsin, and is superimposed on the broad response from the natural abundance ^{13}C in the unsaturated lipids. Fitting of both lines with Lorentzians yields $\omega_{IS}/2\pi = 10\,230 \pm 3$ Hz.

Table 1: Doubly ^{13}C-Labeled Compounds Studied with Their 1-D Rotational Resonance Splittings ($\Delta\omega_1/2\pi$), r_{IS} Distances, and φ, the Torsion over the C10−C20 Part of the Chromophore

doubly ^{13}C-labeled compd	$\Delta\omega_1/2\pi$ (Hz)	r_{IS} (nm)	φ (deg)
[10,20-$^{13}C_2$]-rhodopsin	73 ± 5	0.304 ± 0.015	44
[11,20-$^{13}C_2$]-rhodopsin	83 ± 5	0.293 ± 0.015	44
[10,20-$^{13}C_2$]-10-methylrhodopsin	45 ± 5	0.347 ± 0.015	65
[(10-CH_3),13-$^{13}C_2$]-10-methylrhodopsin	65 ± 5	0.314 ± 0.015	65
[10,20-$^{13}C_2$]-metarhodopsin I	≤ 12	≥ 0.435	0
[10,20-$^{13}C_2$]-metarhodopsin I	93 ± 5	0.283 ± 0.015	0

The off rotational resonance CP/MAS spectrum of [(10-CH_3),13-$^{13}C_2$]-10-methylrhodopsin was also recorded at $\omega_r/2\pi = 10\,000$ Hz. The C10 methyl resonates with $\sigma = 22.0$ ppm. The $^{13}C13$ has $\sigma = 170.8$ ppm and its NMR response is superimposed on the broad natural abundance carbonyl resonances. The $^{13}C13$ signal from the analogue is again shifted 1.9 ppm downfield from the $\sigma = 168.9$ ppm for the C13 response in rhodopsin. From these data a $n = 1$ rotational resonance condition $\omega_r/2\pi = 14953 \pm 3$ Hz was obtained.

Figure 3c represents the vinylic region of the $n = 1$ rotational resonance spectrum of [10,20-$^{13}C_2$]-10-methylrhodopsin. The $\Delta\omega_1$ for [10,20-$^{13}C_2$]-10-methylrhodopsin is smaller than for native [10,20-$^{13}C_2$]-rhodopsin. The corresponding weaker dipolar coupling implies that the C10−C20 distance in 10-methylrhodopsin is larger than for rhodopsin.

The analysis of the second derivatives of the data yields $\Delta\omega_1/2\pi = 45 \pm 7$ Hz for [10,20-$^{13}C_2$]-10-methylrhodopsin and $\Delta\omega_1/2\pi = 65 \pm 7$ Hz for [(10-CH_3),13-$^{13}C_2$]-10-methylrhodopsin. Using eq 1 we obtain $b_{10,20}/(2\pi\sqrt{8}) = 64 \pm 7$ Hz and $b_{(10-CH_3),13}/(2\pi\sqrt{8}) = 87 \pm 7$ Hz, yielding internuclear distances $r_{10,20} = 0.347 \pm 0.015$ nm and $r_{(10-CH_3),13} = 0.314 \pm 0.015$ nm (eq 2 and Table 1).

Metarhodopsin-I. The vinylic regions of the data sets for the illuminated rhodopsin samples are shown in Figure 5. The response from the C10 label was analyzed with Lorentzian line fitting. From the ratio of the integrated response of rhodopsin and metarhodopsin-I, a photoproduct yield of 74% is calculated.

For [10,20-$^{13}C_2$]-metarhodopsin-I (Figure 5a) the C10 resonates with $\sigma = 130.6$ ppm, while the aliphatic C20 response has $\sigma = 13.3$ ppm, yielding $\omega_{IS}/2\pi = 11\,810 \pm 3$ Hz for the $n = 1$ rotational resonance condition. For [11,20-$^{13}C_2$]-metarhodopsin-I (Figure 5b) the C11 response has $\sigma = 139.2$ ppm and the C20 shift is well reproduced, $\sigma = 13.3$ ppm. Lorentzian line fitting of the label signals yields $\omega_{IS}/2\pi = 12\,689 \pm 3$ Hz.

Figure 5c,d depicts the vinylic regions taken from the $n = 1$ rotational resonance spectra of [10,20-$^{13}C_2$]-metarhodop-

sin-I (c) and [11,20-$^{13}C_2$]-metarhodopsin-I (d). In the all-*E* retinylidene chromophore of metarhodopsin-I, the internuclear distance between C10 and C20 is quite large, the dipolar interaction between the labels is weak, and the rotational resonance fine structure is not resolved. In contrast, for the C11 response of metarhodopsin-I at the rotational resonance condition, the splitting due to the dipolar recoupling effect can be observed. To illustrate the fine structure for the C11, the data shown in Figure 4 were processed without apodization.

For the second derivative analysis of the $n = 1$ rotational resonance spectrum of the [11,20-$^{13}C_2$]-metarhodopsin-I the data were reprocessed with 40 Hz apodization. The second derivative spectrum was fitted with second derivative Lorentzians to extract $\Delta\omega_1/2\pi$. An additional second derivative Lorentzian was used in the fitting procedure to account for the C11 response of the doubly labeled rhodopsin residue in the spectrum, which is off resonance. It follows that $\Delta\omega_1/2\pi = 93 \pm 7$ Hz. Using eqs 1 and 2, an $r_{11,20} = 0.283 \pm 0.015$ nm is calculated for the distance between C11 and C20 in metarhodopsin-I (Table 1).

For the [10,20-$^{13}C_2$]-metarhodopsin-I the second derivatives of both the off rotational resonance data and the $n = 1$ rotational resonance data were analyzed with a single second derivative Lorentzian to fit the meta-I response. The excess line width of the C10 resonance due to dipolar recoupling at rotational resonance is a fair estimate of an upper limit for $\Delta\omega_1$ for C10 in metarhodopsin-I. This procedure yields $\Delta\omega_1/2\pi \leq 12$ Hz and $r_{10,20} \geq 0.44$ nm for [10,20-$^{13}C_2$]-metarhodopsin-I (Table 1).

DISCUSSION

Configuration of the Retinylidene Ligand in Rhodopsin. The short $r_{10,20} = 0.304$ nm proves that the retinylidene chromophore in rhodopsin is indeed 11-*Z*-12-*s*-*trans* (*8*, *31*). The splitting at the $n = 1$ rotational resonance condition is resolved for both the ^{13}C10 and the ^{13}C11 response (Figure 3). We have been able to obtain line widths of ~70 Hz before apodization for both [10,20-$^{13}C_2$]- and [11,20-$^{13}C_2$]-rhodopsin, respectively, which compares well with ~45 Hz we typically observe with our spectrometer for pure polycrystalline retinal samples (*16*). This shows that the heterogeneity in the protein is comparable to the variations of the chemical environment in the pure crystals. Hence, the protein environment of both labels may be considered ordered on the scale of the NMR. This is in agreement with the most recent modeling results on the structure of rhodopsins, which converge upon a tight and well-defined packing of the retinal chain between C11 and C14 (*7*, *32*, *33*). The observation of a single rotational resonance pattern for each of the two vinylic labels confirms that both internuclear distances are unique. This effectively excludes the possibility of relating the 0.67 quantum yield to the occurrence of two distinct chromophore conformations, with only one of them photochemically active. It is well in line with recent chiroptical data that provide evidence for one chromophore species with positive helicity (*34*).

Conformation of the Retinylidene Ligand in Rhodopsin. The nonplanarity of the chromophore polyene chain can be characterized in terms of an angle φ between the planes of conjugation on both sides of the 11-*Z* moiety. φ can be estimated starting from the crystal structure of 11-*Z*-12-*s*-*cis*-retinal by rotating around the C12−C13 single bond to match the NMR distance constraints. This yields $\varphi = 44°$, with an error margin of ~10° due to the uncertainties in the distance measurements and the differences in C−C bond distances and C−C−C bond angles between the protonated retinal Schiff base in the protein and the retinal in the crystalline model compound (Table 1). This angle correlates well with the angle of 39° for the C12−C13 bond in crystalline 11-*Z*-12-*s*-*cis*-retinal (*35*) that is thought to be due to steric hindrance between the 10 and the 14 hydrogen. A φ of ~ 44° is also in line with the interpretation of Raman results, solid-state NMR shift restraints, and semiempirical modeling studies (*36*−*38*). In a separate ab initio Car−Parrinello modeling study the structure of the C10−C11═C12−C13−C20 moiety was refined taking into account the delocalization of the torsion (*39*). This suggests that the out-of-plane distortion is distributed over three bonds: C10−C11, C11═C12 and C12−C13, while the angle between the C6−C10 plane of conjugation and the C13−C15 plane is φ ~ 44°. In detail, the minimization converges upon absolute torsional angles of 165° for H−C10−C11−H, −8° for H−C11═C12−H, and 154° for H−C12−C13−C20.

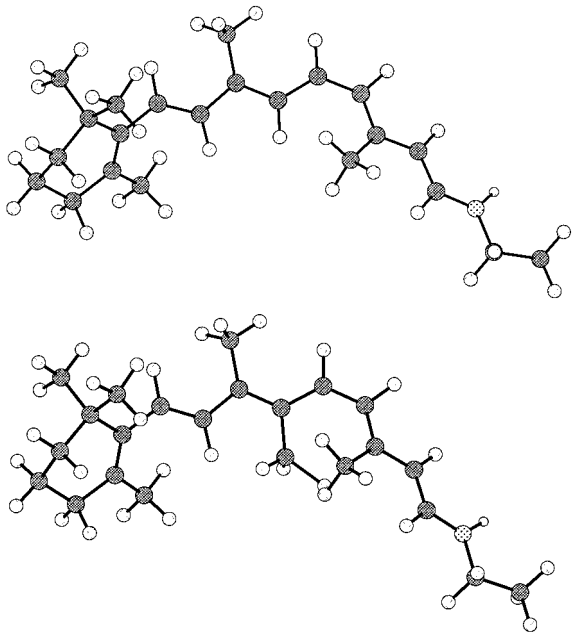

FIGURE 6: Models for (a, top) the retinylidene chromophore in bovine rhodopsin and (b, bottom) its C10 methyl analogue.

The definition of the absolute sense of the rotations was taken in accordance with chiroptical data obtained by Buss et al (*34*). Figure 6a shows the structure of the chromophore based on our distance constraints and model calculations (*37*, *38*). The nonbonding steric interactions force the C13 methyl moiety above the molecular plane and the C10 proton below the plane of the molecule.

This set of conformational distortions is in agreement with the deviation from cis geometry measured recently by Feng et al. (*15*), which probably means an absolute C10−C11 torsional angle of 160 ± 10°.

According to the NMR results, the ligand binding site in rhodopsin should be specific with respect to binding of only one enantiomer. The C13 methyl and the C10 hydrogen bond vectors can be arranged in four possible mutual orientations.

In two of these structures the C13-methyl moiety is on one side of the conjugated plane and the C10 hydrogen is on the opposite side or the other way around. The two remaining alternatives would put both substituents at the same side of the plane of conjugation. Since they lead to pronounced steric interactions and strain in the molecular skeleton, these last two possibilities may be considered unlikely.

The ^{13}C shifts for the labels are close to the values for the corresponding positions in the 11-*Z*-protonated Schiff base (*29*). In particular, there is no indication for γ shift effects due to strong steric hindrance (*32*, *33*). In this respect, the ab initio molecular dynamics calculations using our NMR constraints as a starting point and performed in vacuo appear to confirm that nonbonding steric interactions between the C13 methyl and the C10 hydrogen are not excessively strong (*39*).

Configuration and Conformation of the Ligand in 10-Methylrhodopsin. The isotropic shift of the C10 in 10-methylrhodopsin is 129.2 ppm, which is 1.9 ppm downfield from the C10 shift in rhodopsin. The C20 of 10-methylrhodopsin resonates with $\sigma = 17.4$ ppm and is shifted 1.6 ppm downfield. Like for rhodopsin, there is no evidence for a γ effect induced upfield shift due to spring-loading type effects involving the C20 and the C10-methyl moieties.

For 10-methylrhodopsin $r_{10,20} = 0.347 \pm 0.015$ nm, significantly larger than the 0.304 ± 0.015 nm that was measured for rhodopsin. The internuclear distance between C13 and the 10-methyl moiety is 0.314 ± 0.015 nm. Since $r_{10,20} > r_{(10-CH_3),13}$ for the 10-methyl analogue, the C13 methyl group is pushed out further from the C6−C10 conjugated plane than the C10 CH_3 from the C13−C15 plane. Figure 6b is a picture of the chromophore of 10-methylrhodopsin, which also is 11-*Z*-12-*s*-*trans* according to the intraligand distance constraints. The fact that both 11-*Z*-retinal and 10-methyl-11-*Z*-retinals can bind in the active site of rhodopsin in very similar conformations with subtle structural adjustments that should influence the surrounding protein cage is a nice demonstration of the concept of an induced fit mechanism for ligand protein interactions (*40*, *41*).

Configuration of the Chromophore in Metarhodopsin-I. The 1-D rotational resonance method is new and has been tested previously on small retinal models only. The rhodopsin system offers an interesting possibility for intrinsic validation of the 1-D rotational resonance technology for ligand structure studies, by probing the light-induced configurational change of the chromophore, which has been well-established by other experimental techniques.

The 11,20 $n = 1$ rotational resonance of the [11,20-$^{13}C_2$]-metarhodopsin-I spectrum shows a dipolar recoupling effect with $\Delta\omega_1 = 93 \pm 7$ Hz (Figure 5). This yields $r_{11,20} = 0.283$ nm, close to $r_{11,20} = 0.293$ nm calculated for rhodopsin. Indeed, $r_{11,20}$ is relatively independent of the configuration of the C11═C12 double bond (*42*, *43*). In contrast, the C10−C20 internuclear distance depends strongly on the C11═C12 configuration. In fully planar 11-*Z*-*s*-*trans*-retinal $r_{10,20} = 0.292$ nm, while $r_{10,20} = 0.440$ nm for all-*E* retinal (*42*). This is in agreement with the NMR results, where the rotational resonance spectrum reveals only a marginal broadening ($\leq$12 Hz) of the C10 response, at the $n = 1$ rotational resonance condition. This implies that the $r_{10,20} \geq 0.44$ nm, which matches the $r_{10,20}$ of the all-*E* retinal model. Thus, the intraligand distance measurements strongly suggest that the chromophore, which is thought to be torsionally strained in bathorhodopsin (*44*−*46*) is fully relaxed in the metarhodopsin-I intermediate, in line with FTIR data (*47*, *48*). This is further supported by the chemical shift data, which are a probe for the electronic structure of the chromophore in metarhodopsin-I. The shifts for $^{13}C10$, $^{13}C11$, and $^{13}C20$ are globally in the range reported for model all-*E* retinal protonated Schiff bases (*49*).

Implications for the Visual Process. The presence of methyl substituents in the isomerization region of the polyene chromophore affects the kinetics and quantum yield of the *Z*−*E* isomerization photochemistry (*11*, *50*). Femtosecond absorption experiments show that 9-*Z*-retinal and 11-*Z*-13-demethylretinal chromophores, which lack intramolecular steric interactions involving the 13-methyl group, isomerize on a slower time scale (400−600 fs) than native rhodopsin (*50*, *51*). In addition, the photoisomerization quantum yields in 9-*Z*- and 11-*Z*-13-demethylrhodopsin are lower relative to that of rhodopsin (*11*).

On the basis of these experiments it was proposed that repulsive nonbonding interactions in the chromophore of rhodopsin, associated with steric hindrance between the C13-methyl hydrogens and the C10 hydrogen would lead to an increase of the slope of the reaction coordinate in the Franck−Condon region which should contribute to driving the molecule into an ultrafast and highly efficient *Z*−*E* isomerization process (*50*). This mechanistic model for the isomerization thus relies upon a correlation between the efficiency of the *Z*-*E* isomerization and the magnitude of the out-of-plane deformation of the chromophore. The larger the out-of-plane distortion, the steeper the reaction coordinate and the faster and more efficient the isomerization process.

Quantitative differences between the spatial structure of methyl analogues relative to the native chromophore were not yet resolved experimentally in the past. The NMR distance constraints provide a rigorous structural basis for the photochemistry studies and unambiguous evidence that the nonplanarity of the C10−C11═C12−C13−C20 motif in the 10-methylrhodopsin analogue is larger than for rhodopsin due to the steric interaction between the additional methyl moiety at C10 and the C13 methyl group. Hence, an improvement of the isomerization efficiency of the 10-methyl analogue over the natural system could be expected (*12*, *52*). However, it was recently discovered that the isomerization is less efficient in a rhodopsin analogue with an additional methyl group at the C10. A quantum yield of 0.55 was measured (*12*), compared to 0.67 reported for rhodopsin (*9*, *11*, *50*, *51*). The available data for the photoisomerization quantum yield indicate that the presence of the C13 methyl yields a positive contribution to the photoisomerization quantum yield of $\sim$0.2, essentially independent of the presence of a substituent at C10 or protein perturbations associated with an induced fit, while a methyl substituent at C10 appears to decrease the quantum yield by $\sim$0.12, independent of the presence of a C13 methyl and perturbations of the binding pocket (*12*). Hence the effect of methyl substituents in the polyene region is definitely more complicated than the simple mechanism of increasing the slope of the excited-state surface in the Franck−Condon region suggests.

The binding reaction of 11-*Z*-10-methylretinal with opsin is much slower than for the native chromophore, and the

C10 methyl moiety markedly retards relaxation of the photoisomerized chromophore (*12*). The 10-methylbatho-rhodopsin intermediate is stable up to ~210 K, significantly higher than the batho- to lumirhodopsin transition temperature for rhodopsin (130 K). This suggests a tight binding pocket that serves as a steric complement to the chromophore for the fast isomerization process. A tight binding pocket is also supported by the NMR results. First, the line-widths detected for the label signals are small, in the range for ordered systems. Second, the NMR lines from the labels are quite narrow at low temperature. This puts a constraint on the inhomogeneous broadening due to shift dispersion and indicates that the binding pocket is sufficiently densely packed and sturdy to shield the chromophore from the external stress from the ice matrix surrounding the sample that can easily give rise to substantial inhomogeneous broadening of NMR lines from labels in membrane proteins (*54*, *55*). Third, the 1-D rotational resonance technique requires the detection of detailed fine structure of the vinylic resonances. This should also imply a well-defined and rigid chemical environment of the labels in the ground state of rhodopsin and 10-methylrhodopsin. Hence, all evidence indicates a tight binding pocket. A more loose cavity that e.g., would allow the 13-CH_3 to rotate out of the polyene plane during the photoisomerization process seems unlikely. This suggests a concerted movement over several bonds to accommodate isomerization, with a prominent role for the C12−H hydrogen, and would explain the initial formation of a strained all-*E* configuration highly twisted about single bonds (*39*).

CONCLUSIONS

Obtaining structural data at atomic resolution is an urgent need in membrane protein research, since knowledge about the structure is essential for understanding the molecular processes that control the function of membrane proteins such as receptors, channels, transporters, etc. We present high-resolution structural data for retinylidene ligands bound to their G-protein coupled receptor target in the natural membrane environment. 1-D MAS NMR rotational resonance between two ^{13}C-labeled positions proves to be effective for obtaining internuclear distances and can be used to resolve the spatial structure for specific parts of the chromophore in the active site of rhodopsin. Here, we have used, in particular, the effect of rotor-driven dipolar recoupling on the spectral line shape of the vinylic label response to measure internuclear distances between methyl groups and vinylic carbons. In Table 1 the distance and torsion information for rhodopsin, 10-methylrhodopsin, and metarhodopsin is tabulated.

This already allows us to specify and compare the distortion of the C10−C11═C12−C13−C20 motif in the retinylidene ligand and its C10-methyl analogue. To achieve this, MAS centerband line shapes for the vinylic labels in the 40 kDa intrinsic membrane protein reconstituted with 11-*Z*-[10,20-$^{13}C_2$]- or 11,*Z*-[11,20-$^{13}C_2$]-retinal were measured off and on $n = 1$ rotational resonance, at low temperature (~210 K). Analysis of the second derivatives of the line shape yields $r_{10,20} = 0.304 \pm 0.015$ nm and $r_{11,20} = 0.294 \pm 0.015$ nm. The nonbonding interactions between the C10−H and the C13-methyl moiety provoke an out-of-plane distortion in the isomerization region with an angle $\varphi \sim 44°$ between the C6−C10 and C13−C15 planes of the conjugated chain. It is further concluded that the chromophore of rhodopsin has an ordered structure on the NMR scale. This corroborates evidence that the binding pocket of opsin is tight and selects only one out of four possible enantiomers, with the C10 hydrogen and the C13 methyl moiety on opposite sides of the conjugated chain.

The distance measurements in the chromophore of 10-methylrhodopsin confirm the larger out-of-plane distortion in the isomerization region, provoked by the steric interaction between the C13 and the C10 methyl groups. Assuming that the absolute chirality of the chromophore of 10-methylrhodopsin is identical to that of rhodopsin, the C13 methyl moiety is pushed further above the plane of the conjugated chain of the chromophore.

Finally, the distance measurements in the chromophore of metarhodopsin-I, the third intermediate in the photosequence of the visual pigment, support the overall relaxed all-*E* structure of the chromophore and present additional confirmation for the validity of the 1-D rotational resonance approach for ligand structure refinements.

The NMR results presented in this study provide a structural basis for the studies on photoisomerization kinetics. They support a rhodopsin photochemical isomerization mechanism that operates with a sterically tight binding pocket to provide optimal conditions, in terms of electronic, vibronic, and spatial structure, for a rapid and efficient nonlinear isomerization process, leading to a bathorhodopsin ground state with partial twists in several bonds of the polyene chain and the excess positive charge locked at the Schiff base end due to the electrostatic interaction with the counterion (*39*, *56*, *57*). The isotropic shift of the NMR response of C10 in 10-methylrhodopsin is close to that in the native pigment, which provides strong evidence that the direct effect of the methyl group on the electronic structure, for instance due to the electron-donating properties of the methyl group, is quite small. According to De Lange et al. (*12*), essential features of the vibronic structure observed in the 10-methylrhodopsin to batho FTIR difference spectrum, in particular the strong HOOP modes, indicate a great deal of similarity with the vibronic structure of the native system (*17*). Since the photoisomerization quantum yield for the C10-methyl analogue is less than for the native system, its structural properties may be less favorable for isomerization. In the spatially resolved chromophore structure of Figure 6a the "space" between the C9 and C13 methyls may provide an intramolecular "cavity" that could serve to accommodate the twisting motion of the polyene and the associated hydrogen vibrations or displacements, in particular for H11 and H12 that change configuration from *cis* to *trans*. In contrast, in Figure 6b the C10-methyl partially fills the space between the C9 and C13 methyls, which may act to constrain the C12 isomerization pathway. This leads to the hypothesis that the C9 and C13 methyl groups may contribute to facilitate the polyene isomerization dynamics, while the presence of a methyl group at C10 would represent an additional constraint.

ACKNOWLEDGMENT

The authors wish to thank C. Erkelens and F. Lefeber for technical support. We thank M. H. Levitt for making his simulation programs available.

REFERENCES

1. Birge, R. R. (1990) *Biochim. Biophys. Acta 293*, 1016.
2. Lewis, J. W., and Kliger, D. S. (1992) *J. Bioenerg. Biomembr. 24*, 201.
3. Tang, L., Ebrey, T. G., and Subramaniam, S. (1995) *Isr. J. Chem. 35*, 193.
4. Baldwin, J. (1993) *EMBO J. 12*, 1693.
5. Schertler, G., Villa, C., and Henderson, R. (1993) *Nature 362*, 770.
6. Unger, V., and Schertler, G. (1995) *Biophys. J. 68*, 1776.
7. Han, M., and Smith, S. O. (1995) *Biochemistry 34*, 1425.
8. Hubbard, R., and Kropf, A. (1958) *Proc. Natl. Acad. Sci. U.S.A. 44*, 130.
9. Schoenlein, R. W., Peteanu, L. A., Mathies, R. A., and Shank, C. V. (1991) *Science 254*, 412.
10. Harbison, G. S., Mulder, P. P. J., Pardoen, H., Lugtenburg, J., Herzfeld, J., and Griffin, R. G. (1985) *J. Am. Chem. Soc. 107*, 4810.
11. Kochendoerfer, G. G., Verdegem. P. J. E., van der Hoef, I., Lugtenburg, J., and Mathies, R. A. (1996) *Biochemistry 35*, 16230.
12. De Lange, F., Bovee-Geurts, P. H. M., Van Oostrum, J., Portier, M. D., Verdegem, P. J. E., Lugtenburg, J., and de Grip, W. J. (1997) *Biochemistry 37*, 1411.
13. Creuzet, F., McDermott, A., Gebhard, R., van der Hoef, K., Spijker-Assink, M. B., Herzfeld, J., Lugtenburg, J. Levitt, M., and Griffin, R. G. (1991) *Science 251*, 783.
14. Ulrich, A. S., Wallat, I., Heyn, M. P., and Watts, A. (1995) *Nat. Struct. Biol. 2*, 190.
15. Feng, X., Verdegem, P. J. E., Lee, Y. K., Sandström, D., Edén, M., Bovee-Geurts, P. H. M, de Grip, W. J., Lugtenburg, J., de Groot, H. J. M., and Levitt, M. H. (1997) *J. Am. Chem. Soc. 119*, 6853.
16. Verdegem, P. J. E., Helmle M., Lugtenburg, J., and de Groot, H. J. M. (1997) *J. Am. Chem. Soc. 119*, 169.
17. Groesbeek, M., and Lugtenburg, J. (1992) *J. Photochem. Photobiol. 56*, 903.
18. Verdegem, P. J. E., Monnee, M. C. F., and Lugtenburg, J., submitted to *Eur. J. Org. Chem.*
19. De Grip, W. J., Daemen, F. J. M., and Bonting, S. L. (1980) *Methods Enzymol. 67*, 301.
20. Metz, G., Wu, X., and Smith, S. O. (1994) *J. Magn. Reson. A 110*, 219.
21. Yoshizawa, T., and Wald, G. (1963) *Nature 197*, 1279.
22. Kliger, D. S., and Lewis, J. W. (1995) *Isr. J. Chem. 35*, 289.
23. Peteanu, L. A., Schoenlein, R. W., Wang, Q., Mathies, R. A., and Shank, C. V. (1993) *Proc Natl. Acad. Sci. U.S.A. 90*, 11762.
24. Van Breugel, P. J. G. M., Bovee-Geurts, P. H. M., Daemen, F. J. M., and Bonting, S. L. (1978) *Biochim. Biophys. Acta 509*, 136.
25. De Grip, W. J., Olive, J., and Bovee-Geurts, P. H. M. (1983) *Biochim. Biophys. Acta 734*, 168.
26. Levitt, M. H., Raleigh, D. P., Creuzet, F., and Griffin, R. G. (1990) *J. Chem. Phys. 92*, 6347.
27. Andrew, E. R., Bradbury, A., and Eades, R. G. (1958) *Nature 182*, 1659.
28. Han, M., DeDecker, B., and Smith, S. O. (1993) *Biophys. J. 65*, 899.
29. Smith, S. O., Palings, I., Miley, M. E., Courtin, J., de Groot, H. J. M., Lugtenburg, J., Mathies, R. A., and Griffin, R. G. (1991) *Biochemistry 30*, 1991.
30. Raleigh, D. P., Levitt, M. H., and Griffin, R. G. (1988) *Chem. Phys. Lett. 146*, 71.
31. Wald, G. (1968) *Nature* (*London*) *219*, 800.
32. Shieh, T., Han, M., Sakmar, T. P., and Smith, S. O. (1997) *J. Mol. Biol. 269*, 373.
33. Pogosheva, I. D., Lomize, A. L., and Mosberg, H. I. (1997) *Biophys. J. 70*, 1963.
34. Buss, V., Kolster, K., Terstegen, F., and Vahrenhorst, R. (1998) *Angew. Chem., Int. Ed. Engl. 37*, 1893.
35. Gilarde, R. D., Karle, I. L., and Karle, J. (1972) *Acta Crystallogr. B28*, 2605.
36. Palings, I., van den Berg, E. E. M., Lugtenburg, J., and Mathies, R. A. (1989) *Biochemistry 28*, 1498.
37. Han, M., and Smith, S. O. (1995) *Biophys. Chem. 56*, 23.
38. The torsion around a C1−C2−C3−C4 unit is defined positive as the C2−C3 bond rotates counterclockwise when viewed along the C2−C3 bond.
39. Bifone, A., de Groot, H. J. M., and Buda, F. (1997) *J. Phys. Chem. B 101*, 2954.
40. Koshland, D. E., Jr. (1995) *Angew. Chem. 33*, 2475.
41. Stryer, L. *Biochemistry*, W. H. Freeman & Co., New York.
42. The value for 11-*Z*-12-*s*-*trans*-retinal is derived from the crystal structure of 11-*Z*-12-*s*-*cis*-retinal (see ref. *33*) by simple molecular modeling.
43. Hamanaka, T., and Mitsui, T. (1972) *Acta Crystallogr. B28*, 214.
44. Bagley, K. A., Balogh-Nair, V., Croteau, A. A., Dollinger, G., Ebrey, T. G., Eisenstein, L., Hong, M. K., Nakanishi, K., and Vittitow, J. (1985) *Biochemistry 24*, 6055.
45. Eyring, G., Curry, B., Mathies, R. A., Fransen, R., Palings, I., and Lugtenburg, J. (1980) *Biochemistry 19*, 2410.
46. Eyring, G., Curry, B., Broek, B., Lugtenburg, J., and Mathies, R. A. (1982) *Biochemistry 21*, 384.
47. Siebert, F. (1995) *Isr. J. Chem. 35*, 309.
48. Ganter, U. M., Gärtner, W., and Siebert, F. (1988) *Biochemistry 27*, 7480.
49. Harbison, G. S., Mulder, P. P. J., Pardoen, J. A., Lugtenburg, J., Herzfeld, J., and Griffin, R. G. (1985) *J. Am. Chem. Soc. 107*, 4809.
50. Wang, G., Kochendoerfer, G. G., Schoenlein, R. W., Verdegem, P. J. E., Lugtenburg, J., Mathies, R. A., and Shank, C. V. (1996) *J. Phys. Chem. 100*, 17388.
51. Schoenlein, R. W., Peteanu, L. A., Wang, Q., Mathies, R. A., and Shank, C. V. (1993) *J. Phys Chem. 17*, 12087.
52. Lin, S. W., Groesbeek, M., van der Hoef, I., Verdegem, P. J. E., Lugtenburg, J., and Mathies, R. A. (1998) *J. Phys. Chem. B. 102*, 2787.
53. Ganter, U. M., Schmid, E. D., Perez-Sala, D., Rando, R. R., and Siebert, F. (1990) *Biochemistry 28*, 5954.
54. De Groot, H. J. M., S. O. Courtin, J., van den Berg, E. M. M., Winkel, C., Lugtenburg, J., Herzfeld, J., and Griffin, R. G. (1990) *Biochemistry 29*, 8158.
55. Fischer, M. R., de Groot, H. J. M., Winkel, C., Hoff, A. J., and Lugtenburg, J. (1992) *Biochemistry 31*, 11038.
56. Warshel, A., Chu, Z. T., and Hwang, J. K. (1991) *Chem. Phys. 158*, 303.
57. Smith, S. O., Courtin, J., de Groot, H. J. M., Gebhard, R., and Lugtenburg, J. (1991) *Biochemistry 30*, 7409.

BI983014E